JOURNAL OF THERMOPHYSICS AND HEAT TRANSFER
Vol. 17, No. 3, July–September 2003

Velocity of Sound of Binary Mixture R507 and Ternary Mixture R404A

Jurij Avsec* and Milan Marčič†
University of Maribor, 2000 Maribor, Slovenia
and
Alfred Leipertz‡ and Andreas P. Fröba§
University of Erlangen–Nürnberg, D-91058 Erlangen, Germany

The development of mathematical models for calculation of the velocity of sound and other thermodynamic functions of state for the refrigerant mixtures R507 and R410A is discussed. For the calculation of the thermodynamic functions of state, the perturbation theory with the Lennard–Jones (12-6) potential was used as reference. A model is presented for the calculation of the influence of multipolar, induction, and dispersion interactions. Multipolar interactions are calculated up to octopole moment. All important contributions (translation, rotation, internal rotation, vibration, intermolecular potential energy, and influence of electron and nuclei excitation) are featured. The analytical results are compared with experimental data and models obtained by classical thermodynamics and show quite good agreement. Experimental data have been obtained by dynamic light scattering.

Nomenclature

A	=	free energy
A_A, A_B	=	parts of the free energy, $A_A + A_B$
A^*	=	reduced free energy
c_0	=	velocity of sound
f	=	number of degrees of freedom
H	=	enthalpy
H_H	=	Hamiltonian
$h, \hbar$	=	Planck constant
k_B	=	Boltzmann constant
N	=	number density
p	=	momentum
p_p	=	pressure
R_m	=	universal gas constant
r	=	intermolecular distance
S	=	entropy
T	=	temperature
T^*	=	reduced temperature
u	=	intermolecular potential
V	=	volume
Z	=	parition function
α	=	polarization constant
γ	=	adjustable parameter
$\Delta\omega_M$	=	freuqency shift of the reference light with respect to the frequency of the main beam
ε	=	Lennard–Jones parameter
θ	=	quadropole moment
κ	=	anisotropy of the polarizibility
μ	=	dipole moment
ρ	=	density
ρ^*	=	reduced density
σ	=	Lennard–Jones parameter
Ψ	=	molar concentration
Ω	=	octopole moment

Superscripts and Subscripts

att	=	attraction
conf	=	configuration
disp	=	dispersion
ind	=	induction
pot	=	potential energy
rep	=	repulsion
λ, $\lambda\lambda$, $\lambda\lambda\lambda$	=	first, second, and third order of perturbation

Presented as Paper 2001-2714 at the AIAA 35th Thermophysics Conference, Anaheim, CA, 11–14 June 2001; received 24 May 2002; revision received 30 July 2002; accepted for publication 30 December 2002.

*Assistant Professor, Mechanical Engineer, Department of Thermodynamics, Faculty of Mechanical Engineering. Member AIAA.

†Professor, Mechanical Engineer, Department of Thermodynamics, Faculty of Mechanical Engineering.

‡Professor, Chemical Engineer, Lehrstuhl für Technische Thermodynamik.

§Assistant Professor, Lehrstuhl für Technische Thermodynamik.

Introduction

THE term velocity of sound refers to the velocity of the mechanical longitudinal pressure waves propagation through a medium. It is an important parameter in the study of compressible flow. The calculation of the speed of sound is very important in measurement (acoustic resonance level gauge).[1,2]

After 10 years of research, most of the essential data for all possible relevant substitutes for the fully halogenated hydrocarbons used previously are available. Because of their thermodynamic properties and safety requirements, mixtures are employed in almost all fields of refrigeration and air conditioning. In contrast to the pure substances, data for mixtures from partially fluorinated hydrocarbons are rare. It is not possible to determine experimentally a great number of properties in a large variety of thermodynamic states for these mixtures. Thus, models are employed for the design of apparatus in refrigeration and air conditioning systems.

In engineering practice, refrigeration process calculation is most often carried out by means of charts, diagrams, or predesigned computer programs. Looking for thermodynamic properties using diagrams and charts is extremely time consuming. With computer programs, on the other hand, the time required for data collection is substantially shortened, thus enabling us to calculate properties of some of the most frequently employed refrigerants. However, computer programs allow only the calculation of certain thermodynamic properties, such as entropy, pressure, and enthalpy of a mixture. In practice, we also often use equations of state, obtained through classical thermodynamics. In classical thermodynamics, the thermodynamic properties of state are calculated based on macroscopic observation of substances. The equations obtained by means of classical thermodynamics are empirical and apply only in the region

Table 1 Coefficients for MBWR

i	a_i	b_i	G_i
1	$x_1 T^* + x_2\sqrt{T^*} + x_3 + \frac{x_4}{T^*} + \frac{x_5}{T^{*2}}$	$\frac{x_{20}}{T^{*2}} + \frac{x_{21}}{T^{*3}}$	$\frac{(1-F)}{(2\gamma)}$
2	$x_6 T^* + x_7 + \frac{x_8}{T^*} + \frac{x_9}{T^{*2}}$	$\frac{x_{22}}{T^{*2}} + \frac{x_{23}}{T^{*4}}$	$-\frac{\left(F\rho^{*2} - 2G_1\right)}{(2\gamma)}$
3	$x_{10} T^* + x_{11} + \frac{x_{12}}{T^*}$	$\frac{x_{24}}{T^{*2}} + \frac{x_{25}}{T^{*3}}$	$-\frac{\left(F\rho^{*4} - 4G_2\right)}{(2\gamma)}$
4	x_{13}	$\frac{x_{26}}{T^{*2}} + \frac{x_{27}}{T^{*4}}$	$-\frac{\left(F\rho^{*6} - 6G_3\right)}{(2\gamma)}$
5	$x_{14} T^* + \frac{x_{15}}{T^{*2}}$	$\frac{x_{28}}{T^{*2}} + \frac{x_{29}}{T^{*3}}$	$-\frac{\left(F\rho^{*8} - 8G_4\right)}{(2\gamma)}$
6	$\frac{x_{16}}{T^*}$	$\frac{x_{30}}{T^{*2}} + \frac{x_{31}}{T^{*3}} + \frac{x_{32}}{T^{*4}}$	$-\frac{\left(F\rho^{*10} - 10G_5\right)}{(2\gamma)}$
7	$\frac{x_{17}}{T^*} + \frac{x_{18}}{T^{*2}}$		
8	$\frac{x_{19}}{T^{*2}}$		

under observation. The main drawback of the use of classical thermodynamics is that insight into the microstructure of a substance is lacking. Contrary to classical thermodynamics, with statistical thermodynamics the thermodynamic properties of state on the basis of intermolecular and intramolecular interactions between particles in the same system of molecules can be calculated. Systems composed of a very large number of particles may be dealt with.

In the present paper, we focus on an extended mathematical model based on statistical thermodynamics to provide speed of sound data for pure refrigerants and their mixtures in the vapor phases under saturated conditions. For comparison, an approach based on classical thermodynamics is visited. In the experimental part of this work, the principles of dynamic light scattering (DLS) are briefly introduced. The results provided from this technique for the velocity of sound for the refrigerant mixtures R507 (50 wt% R125 and 50 wt% R143a) and R404A (44 wt% R125, 52 wt% R143a, and 4 wt% R134a) in the vapor phases under saturated conditions are discussed in comparison with different theoretical approaches. Applications of these refrigerants are possible in cold-storage cells, supermarket display cases, ice machines, etc. They are nonflammable. Their zero ozone deoletion potential (Table 1) and very low global warming potential make them interesting ozone friendly refrigerants for applications where hazards can be kept under control.

Classical Thermodynamics

In engineering practice in most cases, thermodynamic tables, diagrams, or different empirical functions obtained from measurement are used (classical thermodynamics). Today, there are numerous equations of state (EOS) reported in the literature for describing the behavior of fluids[3,4]: Van der Waals, Peng–Robinson, Redlich–Kwong, Soave, etc. However, these equations have exhibited some noticeable defects, such as poor agreement with experimental data in undercritical conditions. On the other hand, we can use complex EOS with many constants [Benedict–Webb–Rubin (BWR), Lee–Kessler (see Ref. 2), Benedict–Webb–Rubin–Starling–Nishiumi, Jacobsen–Stewart[5] EOS, Tillner–Roth–Watanabe–Wagner[6] EOS (TRWW), Jacobsen–Lemmon[7] EOS (JL) etc.] These equations are more complicated. They have no insight into the microstructure of matter and poor agreement with experimental data outside the interpolation limits. The calculation of thermodynamic functions of state with the help of classical thermodynamics is well known and will not be described in this paper.

Computation of Thermodynamic Properties of State

To calculate thermodynamic functions of state, we applied the canonical partition function.[6] When the semiclassical formulation for the canonical ensemble for the N indistinguishable molecules is used, the partition function Z can be expressed as follows[1,2,8]:

$$Z = \frac{1}{N!h^{Nf}} \int \cdots \int \exp\left(-\frac{H_H}{k_B T}\right) \cdot \mathrm{d}\boldsymbol{r}_1\, \mathrm{d}\boldsymbol{r}_2, \ldots, \mathrm{d}\boldsymbol{r}_N\, \mathrm{d}\boldsymbol{p}_1\, \mathrm{d}\boldsymbol{p}_2, \ldots, \mathrm{d}\boldsymbol{p}_N \quad (1)$$

where f indicates the number of degrees of freedom of an individual molecule, H is the Hamiltonian molecule system, and vectors $\boldsymbol{r}_1, \boldsymbol{r}_2, \ldots, \boldsymbol{r}_N$ describe the positions of N molecules and $\boldsymbol{p}_1, \boldsymbol{p}_2, \ldots, \boldsymbol{p}_N$ momenta. The canonical ensemble of partition function for the system of N molecules can be expressed by[1,2]

$$Z = Z_0 Z_{\mathrm{trans}} Z_{\mathrm{vib}} Z_{\mathrm{rot}} Z_{\mathrm{ir}} Z_{\mathrm{el}} Z_{\mathrm{nuc}} Z_{\mathrm{conf}} \quad (2)$$

Thus, the partition function Z is a product of terms of the ground state (0), the translation, the vibration, the rotation, the internal rotation, the influence of electron excitation, the influence of nuclei excitation, and the influence of the intermolecular potential energy.

When the canonical theory is used for computing the thermodynamic properties of the state, such as pressure, enthalpy, internal energy, etc., these can be calculated following Refs. 1, 2, and 8.

In this paper, our interest is focused on the calculation of speed of sound. The speed of sound refers to the speed of the mechanical longitudinal pressure waves propagating through a medium.

The propagation of sonic waves for real fluids is in almost all cases nearly isentropic.[9] Therefore, we can calculate the isentropic speed of sound for a real fluid, c_0,

$$c_0 = \sqrt{-V^2 \left(\frac{\partial p_p}{\partial V}\right)_{S,\psi} \frac{1}{M}} \quad (3)$$

where M is the molecular mass and ψ is the molar concentration.

Intermolecular Forces

Molecules are composed of positive and negative charges. According to Coulomb's law of electrostatics, the charges interact, and the interaction energy between the molecules in the system is called intermolecular energy. Hence, we say that intermolecular forces are of electrostatic nature.

The analytical computation of intermolecular potential is extremely complex.[10–16] For certain simple systems, the problem is solvable, although the equations thus obtained are very complicated. This is why further analytical solutions of a configurational integral are exceptionally difficult. In general, the assumption for the sum of repulsive and attractive forces is sufficiently accurate. If the intermolecular potential is denoted by u, then

$$u = u_{\mathrm{rep}} + u_{\mathrm{att}} \quad (4)$$

The occurrence of the repulsive force is associated with the Pauli exclusion principle (see Ref. 8). If two molecules approach one another within a very short distance, so that the electronic clouds of both molecules begin to coincide, certain electrons in the molecules have to move to higher energy levels due to the exclusion principle, made possible only through the supply of sufficient energies, resulting in the occurrence of the repulsive force.

Influence of Lennard–Jones Intermolecular Potential

For a real fluid, it is possible to use the Johnson–Zollweg–Gubbins (JZG) model[15] based on molecular dynamics and Monte Carlo simulations with the Lennard–Jones intermolecular potential. The modified BWR EOS contains 32 linear parameters x_i and one nonlinear parameter γ (Table 1).

Based on Refs. 10 and 15, we can express the configurational free energy A_{conf} as

$$A^*_{\text{conf}} = \sum_{i=1}^{8} \frac{a_i \rho^{*i}}{i} + \sum_{i=1}^{6} b_i G_i \tag{5}$$

where the coefficients a_i, b_i, and G_i are presented in Table 1. Coefficients a_i and b_i are solely functions of the reduced temperature T^*, and the coefficients G_i are functions of the reduced density ρ^* and of the nonlinear adjustable parameter γ:

$$\rho^* = N\sigma^3/V, \qquad T^* = kT/\varepsilon, \qquad A^*_{\text{conf}} = A_{\text{conf}}/N\varepsilon \tag{6}$$

$$F = \exp(-\gamma\rho^{*2}), \qquad \gamma = 3 \tag{7}$$

where A^*_{conf} in Eq. (5) is the reduced configurational free energy.

Impact of Anisotropic Potentials on Thermodynamic Functions of State

There are several methods to compute the influence of anisotropic potentials.[1–22] In the present paper, those models were used that yielded favorable results in practical computations for a large number of components and within a relatively wide range of densities and temperatures.

Lucas–Gubbins Model

The Lucas–Gubbins (LG) model (see Refs. 1, 8, and 23–25) deals with the perturbation expansion around the Lennard–Jones's intermolecular potential. The total intermolecular potential can be written as a sum of the Lennard–Jones (LJ) intermolecular potential and the potential, which also takes into account the orientation of a molecule in space. Using the perturbation expansion around the reference potential, one can then write the configuration effect on the free energy as

$$A_{\text{conf}}/NkT = A^{\text{LJ}}/NkT + A^{\lambda}/NkT + A^{\lambda\lambda}/NkT + A^{\lambda\lambda\lambda}/NkT \tag{8}$$

The free energy of LJ fluid A^{LJ} was calculated using the JZG model.[15]

We consider rigid nonlinear molecules[6] with the assumption that all anisotropic interactions are scalars. The multipole expansion is terminated at the octopole term. Intermolecular repulsion interactions are modeled by the LJ r^{-12} law. The induction interaction is formulated in the isotropic polarizibility approximation. Intermolecular interactions are limited to the second-order term, and cross terms between intemolecular interactions are not considered. The configurational free energy is then given as follows:

First-Order Terms

The inductive forces are

$$(A^{\lambda})^{\text{ind}} = -4\pi N\rho\alpha(\mu^2)[J(6)/\sigma^3] - 6\pi N\rho\alpha(\theta^2)[J(8)/\sigma^5] \tag{9}$$

Second-Order Terms

The multipole forces are

$$(A^{\lambda\lambda})^{\text{mult-mult}} = [A(112)^{\lambda\lambda}]^{\text{mult-mult}} + 2[A(123)^{\lambda\lambda}]^{\text{mult-mult}} + [A(224)^{\lambda\lambda}]^{\text{mult-mult}} \tag{10}$$

$$[A(112)^{\lambda\lambda}]^{\text{mult-mult}} = -\tfrac{2}{3}(\pi N\rho/k_BT)(\mu^4/\sigma^3)J(6) \tag{11}$$

$$[A(123)^{\lambda\lambda}]^{\text{mult-mult}} = -(\pi N\rho/k_BT)(\mu^2\theta^2/\sigma^5)J(8) \tag{12}$$

$$[A(224)^{\lambda\lambda}]^{\text{mult-mult}} = -(14/5)(\pi N\rho/k_BT)(\theta^4/\sigma^7)J(10) \tag{13}$$

If the intermolecular potential is restricted to the dipole–dipole term, Eq. (11) is the only contribution, whereas for quadrupolar molecules (CO_2, C_2H_6, etc.), Eq. (13) is the only nonvanishing term. For tetrahedral molecules (CH_4, CCl_4, CF_4, etc.), the leading multipole term is the octopole–octopole, and the corresponding contribution to free energy is

$$[A(336)^{\lambda\lambda}]^{\text{mult-mult}} = -\frac{19{,}008}{875}\frac{\pi N\rho}{k_BT}\frac{\Omega^4}{\sigma^{11}}J \tag{14}$$

The dispersion forces are

$$[A(202+022)^{\lambda\lambda}]^{\text{disp-disp}} = -\frac{32\pi N\rho}{5k_BT}\sigma^3\varepsilon^2\kappa^2 J(12) - \frac{16\pi^2 N\rho^2}{5k_BT}\varepsilon^2\sigma^6\kappa^2 L(662) \tag{15}$$

$$[A(224)^{\lambda\lambda}]^{\text{disp-disp}} = -\frac{10{,}368\pi N\rho}{875k_BT}\sigma^3\varepsilon^2\kappa^4 J(12) \tag{16}$$

The third-order terms are

$$\left(A^{\lambda\lambda}_A\right)^{\text{mult-mult-mult}} = 3\left[A_A(112;\,112,\,224)^{\lambda\lambda\lambda}\right] + 6\left[A_A(112;\,123;\,213)^{\lambda\lambda\lambda}\right] + 6\left[A_A(123;\,123;\,224)^{\lambda\lambda\lambda}\right] + \left[A_A(224;\,224;\,224)^{\lambda\lambda\lambda}\right] \tag{17}$$

$$\left[A_A(112;\,123;\,213)^{\lambda\lambda\lambda}\right] = \frac{8\pi N\rho}{25(k_BT)^2}\frac{\mu^4\theta^2}{\sigma^8}J(11) \tag{18}$$

$$\left[A_A(112;\,123;\,213)^{\lambda\lambda\lambda}\right] = \frac{8\pi N\rho}{75(k_BT)^2}\frac{\mu^4\theta^2}{\sigma^8}J(11) \tag{19}$$

$$\left[A_A(123;\,123;\,224)^{\lambda\lambda\lambda}\right] = \frac{8\pi N\rho}{35(k_BT)^2}\frac{\mu^2\theta^4}{\sigma^{10}}J(13) \tag{20}$$

$$\left[A_A(224;\,224;\,224)^{\lambda\lambda\lambda}\right] = \frac{144\pi N\rho}{245(k_BT)^2}\frac{\theta^6}{\sigma^{12}}J(15) \tag{21}$$

$$\left(A^{\lambda\lambda}_B\right)^{\text{mult-mult-mult}} = \left[A_B(112;\,112,\,112)^{\lambda\lambda\lambda}\right] + 3\left[A_B(123;\,123;\,224)^{\lambda\lambda\lambda}\right] + 3\left[A_B(123;\,123;\,224)^{\lambda\lambda\lambda}\right] + \left[A_B(224;\,224;\,224)^{\lambda\lambda\lambda}\right] \tag{22}$$

$$\left[A_B(112;\,112;\,112)^{\lambda\lambda\lambda}\right] = \frac{32\pi^3}{135}\left(\frac{14\pi}{5}\right)^{\frac{1}{2}}\frac{N\rho^2}{(k_BT)^2}\frac{\mu^6}{\sigma^3}K(222;\,333) \tag{23}$$

$$\left[A_B(112;\,123;\,123)^{\lambda\lambda\lambda}\right] = \frac{64\pi^3}{315}(3\pi)^{\frac{1}{2}}\frac{N\rho^2}{(k_BT)^2}\frac{\mu^4\theta^2}{\sigma^5}K(233;\,344) \tag{24}$$

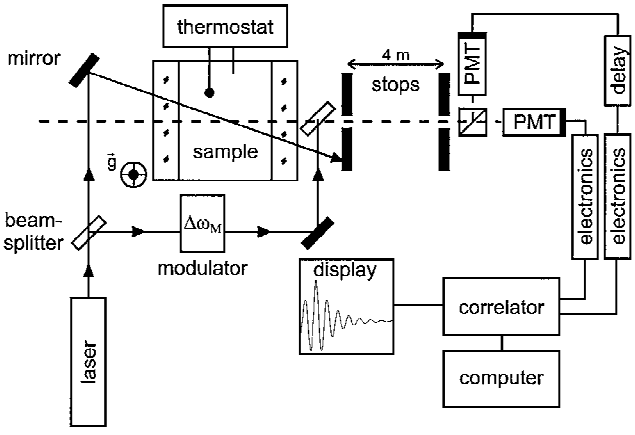

Fig. 1 Experimental setup: optical and electronic arrangement.

$$\left[A_B(123;\,123;\,224)^{\lambda\lambda\lambda}\right] = -\frac{32\pi^3}{45}\left(\frac{22\pi}{63}\right)^{\frac{1}{2}}\frac{N\rho^2}{(k_BT)^2}\frac{\mu^2\theta^4}{\sigma^7}K(334;\,445) \tag{25}$$

$$\left[A_B(224;\,224;\,224)^{\lambda\lambda\lambda}\right] = \frac{32\pi^3}{2025}(2002\pi)^{\frac{1}{2}}\frac{N\rho^2}{(k_BT)^2}\frac{\mu^6}{\sigma^9}K(222;\,333) \tag{26}$$

When intermolecular potential is terminated at the dipole–dipole term, Eq. (23) is the only contributing term. Similarly, for quadrupolar fluids, Eq. (26) is the only nonvanishing term. For tetrahedral molecules where the octopol–octopole potential is the lowest multipole term, $(A_A^{\lambda\lambda\lambda})$ is zero, and we can express the contribution to free energy as

$$\left(A_B^{\lambda\lambda\lambda}\right) = \left[A_B(336;\,336;\,336)^{\lambda\lambda\lambda}\right] - \frac{221{,}184\pi^3}{11{,}375}\left(\frac{3533\pi}{737}\right)^{\frac{1}{2}}\frac{N\rho^2}{(k_BT)^2}\frac{\Omega^6}{\sigma^{15}}K(666,\,777) \tag{27}$$

The structural properties of the LJ potential are introduced via J and K integrals. The J and K integrals are calculated by numerical integration over tabulated pair correlation functions. We calculated J, K, and L integrals with the help of simple interpolation equations presented by Nicolas et al.[25]

In thermodynamic perturbation theory, from the properties of the real system we can obtain the Helmholtz free energy in powers of the perturbation potential [Eq. (15)]. When Eq. (15) is terminated at the third-order term, it is found that the results are good for moderate polar fluids but fail for strong dipoles (H_2O, NH_3, etc.). Similar results have been found for quadrupole forces. This is shown for a liquid state condition in Fig. 1. Because of the slow convergence of Eq. (8) for strong multipole strengths, the following simple Pade approximation for the free energy can be found[25]:

$$A_{\text{conf}}/Nk_BT = A^{\text{LJ}}/Nk_BT + A^{\lambda}/Nk_BT + A^{\lambda\lambda}/Nk_BT\,(1 - A^{\lambda\lambda\lambda}/A^{\lambda\lambda}) \tag{28}$$

Mixing Rules

The thermodynamic properties of LJ mixtures are obtained using one-fluid theory.[23,24] The molecules interacting with the LJ potential have parameters σ and ε given by

$$\sigma^3 = \sum_{\alpha,\beta}\psi_\alpha\psi_\beta\sigma_{\alpha\beta}^3\varepsilon\sigma^3 = \sum_{\alpha,\beta}\psi_\alpha\psi_\beta\varepsilon_{\alpha\beta}\sigma_{\alpha\beta}^3 \tag{29}$$

$$\sigma_{\alpha\beta} = \frac{\sigma_{\alpha\alpha} + \sigma_{\beta\beta}}{2}, \qquad \varepsilon_{\alpha\beta} = \sqrt{\varepsilon_{\alpha\alpha}\varepsilon_{\beta\beta}} \tag{30}$$

The dipole and qudrupole moments are represented[26] as

$$\sigma^3\varepsilon^2\mu^4 = \sum_{\alpha,\beta}\psi_\alpha\psi_\beta\sigma_{\alpha\beta}^3\varepsilon_{\alpha\beta}^2\mu_\alpha^2\mu_\beta^2 \tag{31}$$

$$\sigma^3\varepsilon^2\theta^4 = \sum_{\alpha,\beta}\psi_\alpha\psi_\beta\sigma_{\alpha\beta}^3\varepsilon_{\alpha\beta}^2\theta_\alpha^2\theta_\beta^2 \tag{32}$$

The formulation of the octopole moment is new and is formulated by analogy with dipole and quadrupole moments:

$$\sigma^3\varepsilon^2\Omega^4 = \sum_{\alpha,\beta}\psi_\alpha\psi_\beta\sigma_{\alpha\beta}^3\varepsilon_{\alpha\beta}^2\Omega_\alpha^2\Omega_\beta^2 \tag{33}$$

Experimental Setup

The methodological principles of DLS from bulk fluids are briefly reviewed, and the experimental setup for the determination of the sound velocity is described. For a more detailed and comprehensive description, see, for example, Will and Leipertz[27] and Fröba et al.[28]

When a fluid sample in macroscopic equilibrium is irradiated by coherent laser light, light scattered from the sample can be observed in all directions. The underlying scattering process is governed by microscopic fluctuations of the thermodynamic properties, temperature and pressure, and of species concentrations in fluid mixtures. The relaxation of these statistical fluctuations follows the same laws that are valid for macroscopic systems. Thus, the decay of temperature fluctuations is governed by the thermal diffusivity. Pressure fluctuations in fluids are moving with sound velocity and are damped by the sound attenuation. In fluid mixtures, fluctuations in concentration are decaying in dependence on the mutual diffusion coefficients. In light scattering experiments, the equalization processes result in a temporal modulation of the scattered light intensity. Information about these processes can be derived through a temporal analysis of the scattered light by using photon correlation spectroscopy.

The optical and electrooptical parts of the experimental setup used in this work for the determination of sound velocity are shown at the top of Fig. 1. To perform light scattering from bulk fluids, the scattering volume, which is determined by the intersection of the incident laser beam with the axis of observation (dashed line), is located in the middle of the vessel. An argon ion laser ($\lambda_0 = 488$ nm) was used as a light source. The laser power was up to 300 mW when working far from the critical point and only a few milliwatts in the critical region. A reference beam shifted in frequency by $\Delta\omega_M$ by means of an optoacoustic modulator was added to the scattered light. The scattered light was simultaneously detected by two photomultiplier tubes (PMT) to prevent afterpulsing effects, and the cross-correlation function was calculated by a digital correlator.

According to the specifications of the manufacturer (Solvay), both refrigerant mixtures had a purity of $\geq$99.5% and were used without further purification. The uncertainty in the composition for the binary mixture R507 is certified for each component as $\pm$1 wt%. For the ternary mixture R404A, the uncertainties in the composition are $\pm$2 wt% for R125, $\pm$1 wt% for R143a, and $\pm$2 wt% for R134a. For the present measurements, the samples were placed in a cylindrical pressure vessel (volume about 10 cm^3), which is placed inside an insulated housing. The temperature is regulated through resistance heating and measured by three calibrated 25-Ω platinum resistance probes with an uncertainty of $\pm$0.015 K. The temperature stability was better than $\pm$0.002 K during one experimental run. For each temperature point, typically six measurements at different angles of incidence have been performed. With the experimental setup the saturated vapor sound velocities of the binary and ternary mixtures R507 and R404A, respectively, have been determined with an overall uncertainty being smaller than $\pm$0.5%.

Results and Discussion

We have carried out the calculations for refrigerant mixtures R404A and R507. The comparison of our calculations based on statistical thermodynamics (JZG–LG model) with models obtained based on classical thermodynamics [JL model, TRWW model, and

Table 2 Velocity of sound for R404A at saturated vapor

	c_0, m/s				
T, K	Experiment	JL	S	TRWW	JZG–LG
318.1	122.1	122.7	122.5	122.5	123.3
320.6	120.2	120.4	120.5	120	120.5
323.1	118	118.8	118.4	118.5	118.3
325.7	115.8	116.3	116.1	117.5	116.6
328.1	113.5	114.4	113.8	115.8	114
330.6	111.3	111	111.4	111.3	109.9
333.1	108.4	108.4	109.1	110.9	106.6
335.6	105.6	106.1	107.4	106.4	103.1
AAD, %	——	0.41	0.48	0.93	0.98

Table 3 Velocity of sound c_0 for R507 saturated vapor

	c_0, m/s				
T, K	Experiment	JL	S	TRWW	JZG–LG
315.1	122.14	121.8	121.9	122.5	124.3
317.1	120.98	120.4	120.3	121	122.5
319.1	119.25	118.9	118.7	119.5	120.6
321.1	117.80	117.2	117	117.9	118.5
323.1	116.10	115.5	115.1	116.2	116.2
325.1	113.92	112.8	113.3	114.5	113.8
327.1	112.60	111.8	111.3	112.6	111.2
329.1	110.90	109.9	109.3	110.7	108.4
AAD, %	——	0.58	0.73	0.17	1.05

Table 4 AD for R507 at saturated condition

	AD, %			
T, K	JL	S	TRWW	JZG–LG
315.1	0.278	0.196	0.294	1.768
317.1	0.479	0.562	0.016	1.256
319.1	0.293	0.461	0.209	1.132
321.1	0.509	0.679	0.084	0.594
323.1	0.516	0.861	0.086	0.086
325.1	0.983	0.544	0.509	0.105
327.1	0.710	1.154	0	1.243
329.1	0.171	1.442	0.180	2.254

Solvay package (S)] and experimental results at saturated conditions are presented in Tables 2–4.

Tables 3 and 4 show the average absolute deviation (AAD)

$$\mathrm{AAD} = \sum \left| \frac{(\mathrm{data}_{\mathrm{exp}} - \mathrm{data}_{\mathrm{calc}})}{\mathrm{data}_{\mathrm{exp}}} \right| \Big/ \text{number of points}$$

and absolute deviation (AD)

$$\mathrm{AD} = \left| \frac{(\mathrm{data}_{\mathrm{exp}} - \mathrm{data}_{\mathrm{calc}})}{\mathrm{data}_{\mathrm{exp}}} \right|$$

of the velocity of sound for R507 for the real gas region. The AAD from the experimental data is less than 1% for JL, S, and TRWW models, the JZG–LG model has 1.05% AAD. The best results in comparison with experimental data are obtained by the TRWW model with the maximum AD of 0.3%. The analytical results obtained by statistical thermodynamics show very good agreement with experimental data and with the maximum AD of 2.25%. Somewhat larger deviations can be found in the near critical region due to a larger influence of fluctuation theory and singular behavior of some thermodynamic properties at the near-critical condition.

Tables 2 and 5 show the AAD and AD of the results for R404A between the analytical computation based on the statistical thermodynamics, classical thermodynamics and experimental data. The AAD from the experimental data is less than 1% for the JL, S, TRWW, and JZG–LG models. The best results in comparison with experimental data are obtained by the JL model with the maximum AD of 0.79%.

Table 5 AD for R404A at saturated condition

	AD, %			
T, K	JL	S	TRWW	JZG–LG
318.1	0.491	0.327	0.327	0.982
320.6	0.166	0.249	0.166	0.249
323.1	0.677	0.338	0.423	0.254
325.7	0.431	0.259	1.468	0.690
328.1	0.792	0.264	2.026	0.440
330.6	0.269	0.089	0	1.257
333.1	0	0.645	2.306	1.660
335.6	0.473	1.704	0.757	2.367

The analytical results obtained by statistical thermodynamics (JZG–LG model) show very good agreement with experimental data and have maximum AD of 2.36%. The calculation time required for calculating the velocity of sound based on statistical thermodynamics is practically the same as the time needed for calculating the velocity of sound based on classical thermodynamics.

Conclusions

Calculation of thermodynamic properties of state is possible by use of classical or statistical thermodynamics. Use of classical thermodynamics provides no insight into microstructure, but its use allows the calculation of the thermodynamic function of state with assistance of macroscopic observation of phenomena. Unlike classical thermodynamics, however, use of statistical thermodynamics enables the computation of the thermodynamic functions of the state by studying the molecular structure of the matter.

This paper presents a mathematical model for computation of the velocity of sound in the fluid region based on statistical thermodynamics.

For a real fluid, the JZG model based on molecular dynamics and LJ simulations and modified Benedict–Webb–Rubin equation of state (MBWR) was applied. Multipolar and induction interactions are calculated with the help of quantum mechanical calculation of the intermolecular energy function using LG perturbation theory. The multipole expansion is terminated at the octopole term.

The analytical results are compared with the experimental data obtained by a DLS technique, and they show a very good agreement.

References

[1] Avsec, J., and Marčič, M., "Influence of Multipolar and Induction Interactions on the Speed of Sound," *Journal of Thermophysics and Heat Transfer*, Vol. 14, No. 4, 2000, pp. 496–503.

[2] Avsec, J., and Marčič, M., "Approach for Calculating Thermophysical Properties with the Help of Statistical Thermodynamics," *Journal of Thermophysics and Heat Transfer*, Vol. 16, No. 3, 2002, pp. 455–462.

[3] Tillner-Roth, R., Yokezeki, A., Sato, H., and Watanabe, K., "Thermodynamic Properties of Pure and Blended Hydrofluorocarbon (HFC) Refrigerants," Japan Society of Refrigerating and Air Conditioning Engineers, C3053Y28571E, Tokyo, 1997, Chap. 6.

[4] Walas, S. M., *Phase Equilibria in Chemical Engineering*, Butterworths, Boston, 1984, Chap. 1.

[5] Jacobsen, R. T., Stewart, R. B., Jahangiri, M., and Penoncello, S. G., "A New Fundamental Equation for Thermodynamic Property Correlations," *Advances in Cryogenic Engineering*, Vol. 31, 1986, pp. 1161–1169.

[6] Li, J., Tillner-Roth, R., Sato, H., and Watanabe, K., "Equation of State for HFC Refrigerant Mixtures of HFC-125/143a, HFC-125/134a. HFC-134a/143a and HFC 125/134a/143a," *Fluid Phase Equilibria*, Vol. 161, No. 1, 1999, pp. 225–239.

[7] Lemmon, E. W., and Jacobsen, R. T., "A Generalized Model for the Thermodynamic Properties of Mixtures," *International Journal of Thermophysics*, Vol. 20, No. 3, 1999, pp. 825–835.

[8] Lucas, K., *Applied Statistical Thermodynamics*, Springer-Verlag, New York, 1992, Chaps. 1–6.

[9] Bosnjakovic, F., *Thermodynamics*, Tehnicka Knjiga, Zagreb, Croatia, 1976, Chap. 1.

[10] Moser, B. J., "Die Theorie der Intermolekularen Wechseelwirkungen und Ihre Anwendung auf die Berechnung von Verdampfungsgleichgewichten binärer Systeme," Ph.D. Dissertation, Dept. of Thermodynamics, Univ. Duisburg, Duisburg, Germany, Dec. 1981.

[11] Shukla, K., "Thermodynamic Properties of Binary Mixtures of Atoms and Diatomic Molecules from Computer Simulation and Perturbation Theory," *Fluid Phase Equilibria*, Vol. 127, No. 1, 1997, pp. 1–20.

[12] Shukla, K., "Phase Equilibria and Thermodynamic Properties of Molecular Fluids from Perturbation Theory," *Fluid Phase Equilibria*, Vol. 96, Nos. 1–2, 1994, pp. 19–49.

[12] Margenau, K., and Kestner, N. R., *Theory of Intermolecular Forces*, Pergamon, Oxford, 1969, Chaps. 1–3.

[13] Rigby, M., Smith, E. B., Wakeham, W. A., and Maithland, G. C., *The Forces Between Molecules*, Clarendon, Oxford, 1986.

[14] Gray, C. G., and Gubbins, K. E., *Theory of Molecular Fluids*, Clarendon, Oxford, 1984, Chaps. 1, 2.

[15] Johnson, L. K., Zollweg, J. A., and Gubbins, K. E., "The Lennard–Jones Equation of State Revisited," *Molecular Physics*, Vol. 78, No. 3, 1993, pp. 591–618.

[16] Müller, A., Winkelmann, J., and Fischer, J., "Backone Family of Equations of State: 1. Nonpolar and Polar Pure Fluids," *AIChE Journal*, Vol. 42, No. 4, 1996.

[17] Saeger, B., and Fischer, J., "Construction and Application of Physically Based Equations of State," Pt. 1, *Fluid Phase Equilibria*, Vol. 72, No. 2, 1992, pp. 41–66.

[18] Saeger, B., and Fischer, J., "Construction and Application of Physically Based Equations of State, Pt. 2, *Fluid Phase Equilibria*, Vol. 72, No. 2, 1992, pp. 67–88.

[19] Saeger, B., and Fischer, J., "Construction and Application of Physically Based Equations of State, Pt. 3, Fluid Phase Equilibria, Vol. 93, No. 1, 1994, pp. 101–140.

[20] Lucas, L., Deiters, U., and Gubbins, K. E., "Integrals over Pair- and Triplet-Correlation Functions for the Lennard–Jones (12-6) Fluid," *Molecular Physics*, Vol. 57, No. 2, 1986, pp. 241–253.

[21] Guevara, A. L., and Benavides del Rio, F., "Thermodynamics of a Square-Well Octopolar Fluid," *Molecular Physics*, Vol. 89, No. 5, 1996, pp. 1277–1290.

[22] Strogyn, D. E., "Third Virial Coefficients of Nonspherical Molecules," *Journal of Chemical Physics*, Vol. 30, No. 11, 1969, pp. 4269–4986.

[23] Twu, C., and Gubbins, K. E., "Thermodynamic of Polyatomic Fluid Mixtures," *Chemical Engineering Science*, Pt. 2, Vol. 33, 1978, pp. 879–887.

[24] Twu, C., and Gubbins, K. E., "Thermodynamics of Polyatomic Fluid Mixtures," *Chemical Engineering Science*, Pt. 1, Vol. 33, 1978, pp. 863–878.

[25] Nicolas, J. J., Gubbins, K. E., Street, W. B., and Tildesley, D. J., "Equation of State for Lennard–Jones fluid," *Molecular Physics*, Vol. 37, No. 5, 1979, pp. 1429–1454.

[26] Weingerl, U., Wedland, M., Fischer, J., Müller, A., and Winkelman, J., "Backone Family of Equations of State: 2. Nonpolar and Polar Fluid Mixtures," *AIChE Journal*, Vol. 47. No. 3, 2001, pp. 705–717.

[27] Will, S., and Leipertz, A., "Thermophysical Properties of Fluids from Dynamic Light Scattering," *International Journal of Thermophysics*, Vol. 22, No. 1, 2001, pp. 317–338.

[28] Fröba, A. P., Will, S., and Leipertz, A., "Thermophysical Properties of Binary and Ternary Mixtures from Dynamic Light Scattering," *International Journal of Thermophysics*, Vol. 22, No. 5, 2001, pp. 1349–1368.